

pubs.acs.org/macroletters Letter

¹ Free Energy Trajectory for Escape of a Single Chain from a Diblock ² Copolymer Micelle

3 Sarah C. Seeger, Kevin D. Dorfman,* and Timothy P. Lodge*



Cite This: https://doi.org/10.1021/acsmacrolett.1c00508



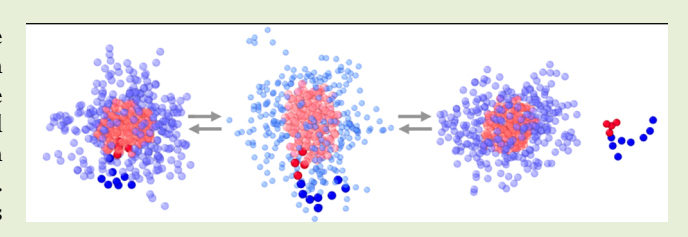
ACCESS |

III Metrics & More

Article Recommendations

Supporting Information

4 **ABSTRACT:** We use umbrella sampling to compute the free 5 energy trajectory of a single chain undergoing expulsion from an 6 isolated diblock copolymer micelle. This approach elucidates the 7 experimentally unobservable transition state, identifies the spatial 8 position of the maximum free energy, and reveals the chain 9 conformation of a single chain as it undergoes expulsion. 10 Combining umbrella sampling with dissipative particle dynamics 11 simulations of A_4B_8 micelles reveals that the core block (A) of the



12 expelled chain remains partially stretched at the transition state, in contrast with the collapsed state assumed in some previous 13 models. The free energy barrier increases linearly with the Flory–Huggins interaction parameter χ up to large interaction energies, 14 where the structure of the otherwise spherical core apparently deforms near the transition state.

The self-assembly of block copolymers into micelles is essential for a variety of applications, including viscosity modification of oils, ^{1,2} the formation of complex block polymer phases, ³ and controlled drug release. ⁴⁻⁶ Many of these applications require micelles to maintain a dynamic equilibrium. Importantly, chain exchange is a fundamental process of micelle relaxation which has been shown theoretically to be the dominant mechanism close to equilibrium. ^{7,8} However, despite substantial experimental progress, an understanding of the molecular level details of the process remains incomplete.

Experimentally, chain exchange has been studied with 26 fluorescence spectroscopy, 9,10 stopped-flow techniques, 11–13 27 and more recently time-resolved small-angle neutron scattering (SANS).14-26 All of these methods provide information about 29 the kinetics of chain exchange for the system ensemble and 30 cannot directly probe the transition state. In the case of SANS, 31 the free energy barrier to chain expulsion, assumed to be the 32 rate-limiting step for chain exchange, 8 can be obtained from 33 the measured time constant for exchange, $\tau_{\rm ex}$ either by 34 examining the temperature dependence of au_{ex} or by fitting to a 35 model. The position of the transition state along the "reaction 36 coordinate" should provide insight into the conformation of 37 the block copolymer chain as it undergoes expulsion from the 38 micelle; however, the full free energy profile for chain exchange 39 has only been computed for small-molecule surfactant 40 systems.²⁷ Most exchange experiments have been interpreted 41 in the context of the theory of Halperin and Alexander, which 42 describes the process of chain expulsion for block copolymer 43 micelles by assuming that the core block collapses into a 44 globule upon entering the corona. In this theory, their model 45 for the transition state that leads to a free energy barrier scales 46 as $\gamma N_{\rm A}^{2/3}$, where γ is the interfacial energy between the core 47 block and the solvent and $N_{\rm A}$ is the core block degree of polymerization. Recent studies have found the barrier to scale 48 linearly with $N_{\rm A}^{14,15,17,34}$ casting doubt on the postulated 49 transition state by Halperin and Alexander. The same linear 50 dependence was also reported in the barrier from measure- 51 ments of chain diffusion in ordered block copolymer 52 melts. These results raise the possibility that a core 53 block is not significantly collapsed upon entering the 54 unfavorable domain. As the resolution of experimental 55 techniques is not yet sufficient to yield information about 56 the conformation of single chains undergoing expulsion, there 57 remains a need to develop simulation techniques to access the 58 core block conformation at the transition state for chain 59 exchange.

In this work, we introduce a simulation framework to 61 evaluate the nature of the transition state to chain exchange 62 and thus the foundations of the Halperin and Alexander model. 63 Here, we employ an umbrella sampling method to compute 64 the free energy landscape for a chain undergoing expulsion 65 from a spherical micelle. We utilize a model dissipative particle 66 dynamics 31,32 (DPD) system of coarse-grained 44 B₈ block 67 polymers in dilute solution, a system originally studied by Li 68 and Dormidontova and others. $^{33-35}$ Notably, we expect this 69 model to provide information about chain exchange despite 70 lacking molecular-level details because the experimental 71 results 14,15,17 are independent of the polymer system. DPD 72

Received: August 5, 2021 Accepted: November 17, 2021



73 uses soft potentials for bead-bead repulsion, which do not 74 capture in detail steric interactions but provide fast 75 equilibration that is desirable for our work. We do not expect 76 the approximations in DPD to impact the key results. Our 77 micelles have amorphous, roughly spherical cores, so the 78 impact of steric interactions on the structure of the micelle 79 core will not play a role here. The most likely impact of the soft 80 DPD potential is to allow chain crossing, which produces 81 dynamics that are faster than expected in an experiment with 82 an entangled micelle core. Since we examine the thermody-83 namics rather than kinetics, this does not impact our results. 84 Moreover, experiments of interest 17 use molar masses that are 85 low enough that the core blocks are not entangled, rendering 86 the chain crossing a minor issue. Finally, although this level of 87 coarse graining cannot resolve the globule hypothesis due to 88 limitations in excluded volume and chain length, it provides a 89 necessary first step toward understanding the behavior of single 90 chains undergoing expulsion.

In this model, monomer beads of mass m are linked by a paramonic bond with equilibrium distance $r_0 = d_p$ and force so constant $k = 100k_BT/d_p^2$; k_BT and d_p are units for energy and distance, respectively. The solvent (S) is modeled by single B-95 type monomer beads. Characteristic of the DPD model, the interaction force between beads is the pairwise sum of a conservative force, f_C , a random force describing thermal gluctuations, f_R , and a dissipative or frictional force, f_D , which acts as a thermostat to conserve the system energy.

The functional forms of these forces are described 101 elsewhere; 31,32 they are short-ranged with a cutoff distance r_c $_{102} = d_{\rm p}$. Similar to previous work, $_{33,34}$ a frictional force with magnitude $\xi = 3.0k_{\rm B}T/d_{\rm p}^2$ and a time step $\Delta t = 0.04~(md_{\rm p}^2/m^2)$ $k_{\rm B}T)^{1/2}$ were used. In these simulations, 81 000 beads were 105 placed randomly in a cubic box of side $30d_p$ with a polymer 106 volume fraction $\varphi = 0.05$. Periodic boundary conditions were 107 implemented, and the repulsive interaction parameter for like 108 particles, $a_{AA} = a_{BB} = a_{BS}$, was set to $25k_BT/d_p^{2.32}$ In the 109 following, we omit the units of k_BT/d_p^{2} for conciseness. The 110 system was equilibrated for a value of excess interaction energy 111 for contacts between A and B beads ($\Delta a = a_{AB} - a_{AA}$) of 15 by 112 slowly increasing Δa and monitoring the system until the aggregation numbers were stable ($t \approx 10^6$, or 2.5×10^7 steps). 114 The system was then placed in the strong segregation regime, 115 where the excess interaction energy was then set to larger 116 values from 22.5 to 40 to halt chain exchange during the 117 umbrella sampling procedure, essentially freezing the distribu-118 tion of aggregation numbers Q. Importantly, we use larger 119 values of Δa than past simulations of chain exchange 120 kinetics, 33,34 which were limited to lower interaction energies 121 to allow micelles to equilibrate within a reasonable simulation 122 time. Our work is intended to mimic experimental systems, in 123 which micelles often cannot fully equilibrate as the necessary 124 relaxation processes are too slow. 18,21,36,37

A single aggregate was selected for umbrella sampling from the frozen micellar system at the designated interaction energy. First, a cluster analysis using a cutoff distance between core beads of 1.8 was performed to find the distribution of aggregation numbers Q^{33} . A locally equilibrated micelle was then chosen with Q = 36, which was always within 10% of the weight-average aggregation number of the frozen Q^{33} distribution, and all other micelles in the system were replaced by solvent beads. Notably, Q = 36 would likely be below the global equilibrium aggregation number Q_{eq} for the system. It is possible to determine Q_{eq} by computing the escape free energy

as a function of micelle size; ⁴⁵ however, it is not necessary for ¹³⁶ our micelle to be at equilibrium as we are interested in the ¹³⁷ single-chain behavior rather than the system ensemble. ¹³⁸ Following Halperin and Alexander, ⁸ the reaction coordinate r ¹³⁹ was defined as the distance between the center-of-mass of the ¹⁴⁰ micelle core and the position of the A-B chain junction. As ¹⁴¹ shown in Figure 1, a harmonic force with k = 12.0 was exerted ¹⁴² fi

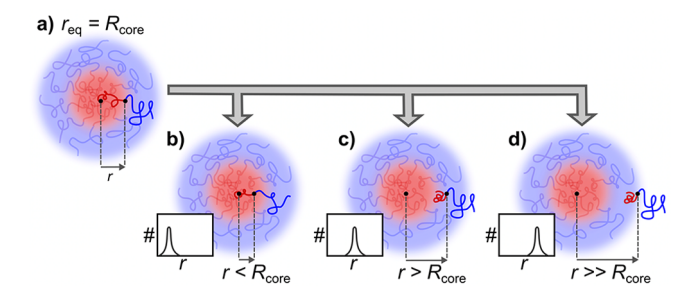


Figure 1. Schematic of the umbrella sampling procedure. (a) The equilibrium state of a micelle and the beginning point of the umbrella sample. (b-d) Separated simulations with biasing potentials added to hold the junction of the chain (b) closer to the micelle center-of-mass than is likely at equilibrium, (c) slightly further away than the equilibrium state, and (d) at a much larger distance than the equilibrium state. Insets in (b-d): Schematic of the number of points in the simulation that have approximately a distance r between the micelle center-of-mass and the biased chain center-of-mass.

via the *colvars* module³⁸ in LAMMPS³⁹ to bias the system such 143 that a randomly chosen chain was held at a selected distance 144 away from the micelle center-of-mass. If another chain 145 exchange event occurred during the course of the umbrella 146 sampling window, the data were discarded due to an incorrect 147 center-of-mass calculation, and the simulation was repeated. 148 The value of the reaction coordinate r was calculated every 10^3 149 time steps, and distances for subsequent umbrella windows 150 were chosen such that the resulting histograms overlapped and 151 the simulations yielded information for all observable distances 152 of r, as illustrated in Figure 2. These histograms were shown to 153 f2 be self-consistent, as determined by a procedure derived from 154 the Kolmogorov–Smirnov test (Figure S1), 40 indicating that 155

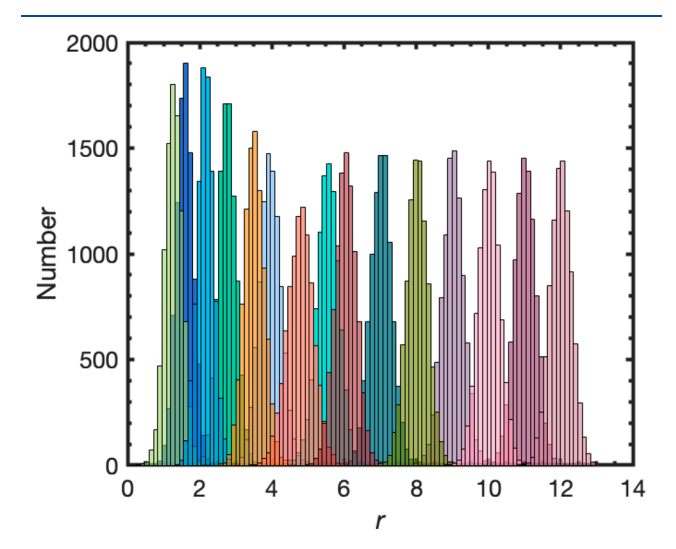


Figure 2. Histograms of observed values of the reaction coordinate r over the course of the simulation for $\Delta a = 25$. Each color represents a different umbrella window.

156 our sampling was sufficient. The potential of mean force was 157 extracted from the observed histograms through the weighted 158 histogram analysis method (WHAM), 41,42 similar to what has 159 been done in hydration studies of proteins. 43 The results were 160 shown to be insensitive to the number of histograms (Figure 161 S2), and error analysis was performed via bootstrapping. The 162 simulation trajectories were confirmed to be reversible by a 163 reverse pulling simulation (Figure S3) as performed for past 164 simulations of surfactant micelles.

Figure 3 shows that there is a sharp increase in free energy as 166 the chain junction departs from the core—corona interface at *r*

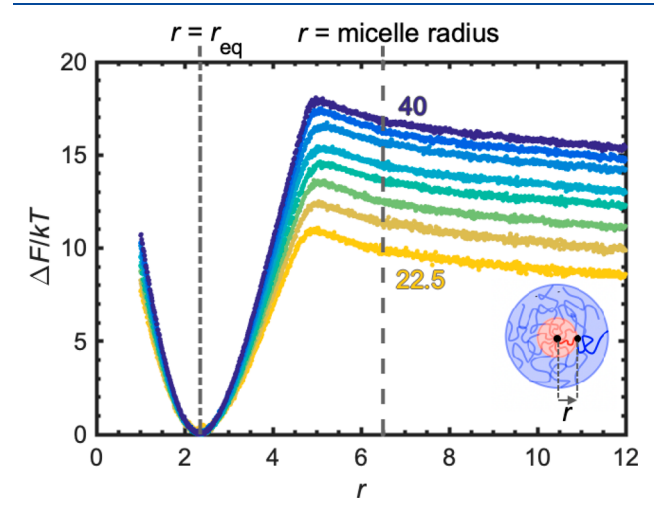


Figure 3. Free energy profiles of chain expulsion from a micelle with Q = 36 as a function of the distance between the center-of-mass of the micelle and the junction of the chain being expelled (r). From bottom to top: Δa ranges from 22.5 to 40 in increments of 2.5. The dash—dot line designates the average distance around equilibrium, and the dashed line is the approximate outer radius of the micelle, i.e., the extent of the micelle corona.

 $_{167}\approx 2.35$ (the zero-free-energy or reference state). Below the equilibrium value of r, the corona block is pulled into the core log along with the chain junction, and the unfavorable contacts to between the core and corona beads result in an increase in internal energy of the system. Similarly, as the distance between the chain junction and micelle center-of-mass increases, the interaction between the core beads and the solvated corona beads adds an internal energy penalty. In this case, however, corona crowding adds an additional entropic penalty. The point of highest free energy, designated the transition state, occurs near a value $r^*\approx 5.0$ in all cases, recalling that all micelles have the same aggregation number and therefore the same core radius.

To compare the results in Figure 3 to experiment, we 181 applied Kramers' rate theory to the computed free energy 182 profiles. Here, we converted from DPD to real units using $R_{\rm core}$ 183 ~ 90 Å and $D \sim 10^{-11}$ cm²/s as calculated from the Rouse 184 model, taking experiments by Choi et al. as a model system. ⁴⁶ 185 We found a time scale of chain exchange on the order of 186 minutes to days for varying Δa (Figure S4). This is similar to 187 the observed experimental chain exchange times, an encourag-188 ing result given that this analysis is far from a rigorous 189 comparison.

To analyze the core chain conformation at the transition 191 state, we calculated the radius of gyration, $R_{\rm g}$, for the perturbed 192 core chain as a function of r. Here, we isolate the data for $\Delta a =$

25; however, the same trend holds for all interaction energies 193 studied (see the Supporting Information for other values of 194 Δa). As seen in Figure 4, the radius of gyration initially 195 f4

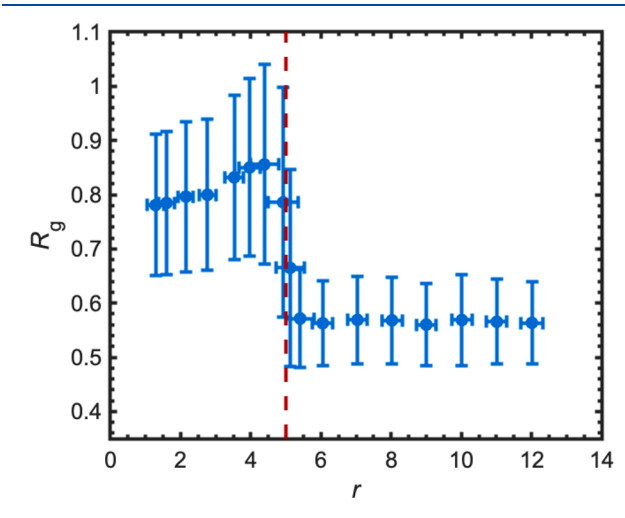


Figure 4. Radius of gyration of the core block along the reaction coordinate for chain expulsion, the distance between the center-of-mass of the micelle, and the junction of the chain being expelled. Each point represents one umbrella window. Error bars are the standard deviation for observations over the course of the umbrella sample.

increases as the chain is being expelled, likely due to chain 196 stretching as part of the chain remains in the core to minimize 197 the internal energy penalty of exposure to corona. The radius 198 of gyration begins to rapidly decrease as r is increased beyond 199 the transition state. Notably, however, the core chain is still 200 partially expanded at the transition state, but the radius of 201 gyration decreases to its minimum while the chain junction is 202 within the micelle corona, which extends to $r \approx 6.5$. This 203 system with $N_A = 4$ is too small to collapse completely to form 204 a globule, however, consistent with prior DPD work. 47 This is 205 a limitation of this model system and indicates that we cannot 206 really assess the validity of the postulated globular transition 207 state. The observed transition state, where the perturbed core 208 block stretches to remain partially shielded in the spherical 209 core, does not necessarily reflect what occurs in solutions of 210 longer chains that fully collapse in a bad solvent. In the future, 211 we plan to use this technique to examine micelles with longer 212 chains to address this important point.

It is evident that both the free energy increase upon chain 214 expulsion and the height of the barrier are strongly dependent 215 on the excess interaction energy Δa , as a higher interfacial 216 energy leads to a larger enthalpic penalty for exposure of core 217 beads to solvent. Figure 5a shows that the height of the free 218 f5 energy barrier in Figure 3 increases approximately linearly with 219 Δa , with a slope of 0.43. Here, we can conclude that an 220 increase in Δa or χ will yield a monotonic increase in the free 221 energy barrier. Notably, there is a slight deviation from the 222 linear trend at high interaction energies ($\Delta a \geq 40$). It is 223 possible that this difference is due to the deformation of the 224 micelle core at the transition state seen in the inset of Figure 225 5a. Although the unperturbed micelle remains spherical at Δa 226 = 40, the micelle core distorts near the transition state to 227 accommodate the displacement of the core block. This reduces 228 the energetic penalty of exposure of core beads to the micelle 229 core even as it extends toward the transition state.

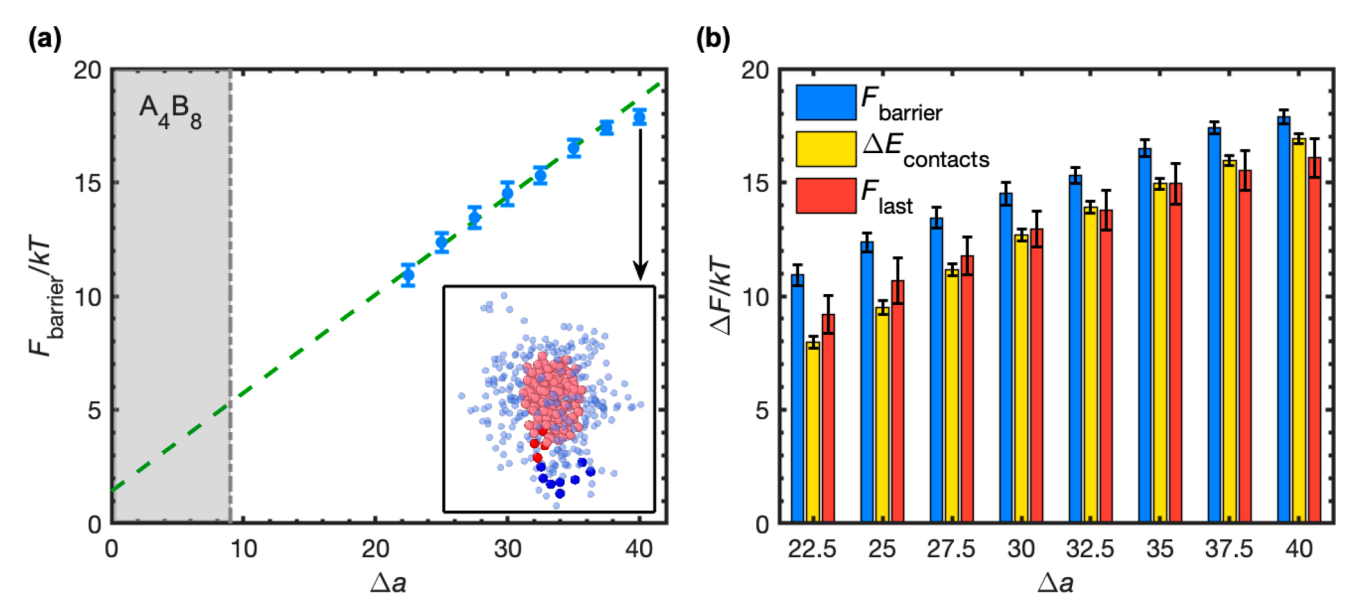


Figure 5. Effect of interaction energy on free energy contributions to chain expulsion. (a) Blue points designate the free energy barrier for chain exchange, with the dashed line indicating a linear fit to the first 6 points. The gray dashed line marks the approximate boundary beyond which micelles do not form. Inset: Configuration of a micelle close to the transition state for the largest interaction energy case ($\Delta a = 40$), rendered by VMD (solvent beads are omitted). Core beads are shown in red and corona beads in blue. Transparency is decreased for the chain being expelled. (b) Yellow bars represent the increase in energy due solely to contacts of the core block with solvent upon expulsion, and red indicates the change in free energy once the chain is fully expelled from the micelle compared to the minimum free energy state.

A second point is that the extrapolated barrier for Δa or $\chi =$ 231 232 0 from the data in Figure 5a is positive, where we would expect 233 the barrier to be zero if there were no excess interaction energy 234 for A-B contacts. In fact, Ma and Lodge, 15 and later Wang et 235 al., ²⁰ discussed a possible offset from a zero free energy barrier 236 at $\chi = 0$, as no micelles should form for a block polymer where 237 the core block is at, or above, the theta point ($\chi \geq 0.5$). Thus, 238 there is reason to expect that the barrier might not remain 239 linear in Δa as the demicellization transition is approached. 240 Note also that the extrapolation is substantial, as the umbrella sampling method can only be implemented at large Δa values 242 where chain exchange is rare. Additionally, the simulations are 243 intended to mimic the experimental situation for many block copolymer micelles, which tend not to be in equilibrium. In a system with larger excess free energy, the equilibrium 246 aggregation number is expected to increase, but the current 247 system is frozen at lower Q.

The free energy barrier to chain exchange ranges from 11 to 249 18 kT with increasing interaction energy. To resolve the 250 contribution that is due to an increase in energy, we examined 251 the increase in energy due to contacts of the core block upon 252 expulsion into the solvent. Here, the energy due to pairwise 253 contacts in each case (as a free chain and within the micelle) is 254 calculated as

$$E_{\text{core}} = \sum_{i=1}^{N_{A}} \sum_{j=1}^{N} E_{ij}$$
(1)

256 where

$$E_{ij} = \begin{cases} \frac{a_{ij}}{2} (1 - r_{ij})^2 & r_{ij} < 1\\ 0 & r_{ij} \ge 1 \end{cases}$$
(2)

258 where N is the number of beads and r_{ij} is the distance between 259 beads i and j. The excess energy due to contacts, $\Delta E_{\rm contacts}$ or

 $E_{\rm core,micelle}-E_{\rm core,free}$, is displayed in Figure 5b. For comparison, 260 the increase in free energy at large values of r (designated $F_{\rm last}$ 261 in Figure 5b), where the chain is fully expelled, is also shown. 262 This increase in free energy, compared to the reference state 263 where the chain junction lies at the core—corona interface, 264 reflects the combined effects of a relief of corona stretching 265 and the energetic penalty of the free chain in solution as well as 266 a change in free energy per chain for the micelle as Q is 267 decreased.

From Figure 5b, it is clear that $\Delta E_{\text{contacts}}$ accounts for the 269 large majority of the free energy barrier to chain expulsion. 270 This contribution increases with interaction energy, from 73% 271 for $\Delta a = 22.5$ to 94% for $\Delta a = 40$. This is likely because the 272 other main contribution to the free energy barrier is due to 273 chain stretching at the transition state, which should not be 274 strongly dependent on interaction energy for micelle cores that 275 remain spherical at the transition state. Moreover, we find that 276 $\Delta E_{
m contacts}$ is not significantly different from $F_{
m last}$ supporting the 277 conclusion that an increase in entropy due the relief of corona 278 chain stretching is a relatively minor contribution to the total 279 change in free energy. We do note that the chosen aggregation 280 number of Q = 36 is likely to be below the optimal aggregation 281 number for this system and for most experimental systems, and 282 one should therefore expect an additional increase in free 283 energy per chain of the micelle upon expulsion because the 284 ensemble is moving further away from equilibrium.

In summary, this work demonstrates that umbrella sampling 286 can be used to compute the free energy profile for chain 287 expulsion in a block copolymer micelle. As the chain is expelled 288 through the corona, the core block initially stretches until it 289 begins to shrink at the transition state due to internal energy 290 considerations. The free energy barrier to chain exchange was 291 found to increase linearly with the Flory–Huggins interaction 292 parameter χ , validating past experimental and theoretical 293 results; however, at large interaction penalties, the transition 294 state may involve a deformation of the micelle core, causing a 295

296 deviation from this linear trend. This work provides insight 297 into the behavior of single chains during expulsion from block 298 polymer micelles and a pathway for future studies evaluating 299 discrepancies surrounding the process of single-chain exchange 300 and the proposed transition state.

ASSOCIATED CONTENT

302 Supporting Information

303 The Supporting Information is available free of charge at 304 https://pubs.acs.org/doi/10.1021/acsmacrolett.1c00508.

> Test of histogram sampling, reverse pulling simulations confirming the reversibility of umbrella sampling trajectories, histogram consistency test, and details on the core chain radius of gyration as a function of the reaction coordinate at other interaction energies (PDF)

AUTHOR INFORMATION 310

311 Corresponding Authors

Timothy P. Lodge - Department of Chemical Engineering 312 and Materials Science, University of Minnesota - Twin 313 Cities, Minneapolis, Minnesota 55455, United States; 314 Department of Chemistry, University of Minnesota - Twin 315 Cities, Minneapolis, Minnesota 55455, United States; 316 orcid.org/0000-0001-5916-8834; Email: lodge@ 317 318

Kevin D. Dorfman – Department of Chemical Engineering and Materials Science, University of Minnesota - Twin Cities, Minneapolis, Minnesota 55455, United States; orcid.org/0000-0003-0065-5157; Email: dorfman@ umn.edu

324 Author

305

306

307

308

319

320

321

322

323

Sarah C. Seeger - Department of Chemical Engineering and 325 Materials Science, University of Minnesota - Twin Cities, 326 Minneapolis, Minnesota 55455, United States 327

328 Complete contact information is available at:

329 https://pubs.acs.org/10.1021/acsmacrolett.1c00508

330 Notes

331 The authors declare no competing financial interest.

332 ACKNOWLEDGMENTS

333 This work was supported by the National Science Foundation 334 Polymers Program (DMR-1707578 and DMR-2103630) and 335 by an NSF Graduate Research Fellowship (S.C.S.). The 336 authors acknowledge the Minnesota Supercomputing Institute 337 (MSI) at the University of Minnesota for providing resources 338 to perform the simulations in this work and Vaidyanathan 339 Sethuraman for helpful discussions surrounding this work.

340 REFERENCES

- (1) Anderson, W. Block Copolymers as Viscosity Index Improvers for 342 Lubrication Oils; 1973, 3763044.
- (2) Stambaugh, R. L.; Kinker, B. G. Viscosity Index Improvers and 344 Thickeners BT. In Chemistry and Technology of Lubricants; Mortier, R. 345 M., Fox, M. F., Orszulik, S. T., Eds.; Springer: Netherlands, 2010; pp 346 153-187.
- (3) Lewis, R. M.; Arora, A.; Beech, H. K.; Lee, B.; Lindsay, A. P.; 348 Lodge, T. P.; Dorfman, K. D.; Bates, F. S. Role of Chain Length in the 349 Formation of Frank-Kasper Phases in Diblock Copolymers. Phys. Rev. 350 Lett. 2018, 121 (20), 208002.
- (4) Hubbell, J. A. Enhancing Drug Function. Science 2003, 300 352 (5619), 595–596.

- (5) Kazunori, K.; Glenn, S. K.; Masayuki, Y.; Teruo, O.; Yasuhisa, S. 353 Block Copolymer Micelles as Vehicles for Drug Delivery. J. Controlled 354 Release 1993, 24 (1-3), 119-132.
- (6) Luo, L.; Tam, J.; Maysinger, D.; Eisenberg, A. Cellular 356 Internalization of Poly(Ethylene Oxide)- b -Poly(ε-Caprolactone) 357 Diblock Copolymer Micelles. Bioconjugate Chem. 2002, 13 (6), 358 1259-1265.
- (7) Aniansson, E. A. G.; Wall, S. N. Kinetics of Step-Wise Micelle 360 Association. J. Phys. Chem. 1974, 78 (10), 1024-1030.

361

- (8) Halperin, A.; Alexander, S. Polymeric Micelles: Their Relaxation 362 Kinetics. Macromolecules 1989, 22 (5), 2403-2412.
- (9) Creutz, S.; van Stam, J.; de Schryver, F. C.; Jérôme, R. Dynamics 364 of Poly((Dimethylamino)Alkyl Methacrylate-Block-Sodium Metha- 365 crylate) Micelles. Influence of Hydrophobicity and Molecular 366 Architecture on the Exchange Rate of Copolymer Molecules. 367 Macromolecules 1998, 31, 681-689. 368
- (10) Cao, T.; Munk, P.; Ramireddy, C.; Tuzar, Z.; Webber, S. E. 369 Fluorescence Studies of Amphiphilic Poly(Methacrylic Acid)-Block- 370 Polystyrene-Block-Poly(Methacrylic Acid) Micelles. Macromolecules 371 1991, 24, 6300-6305.
- (11) Bednar, B.; Edwards, K.; Almgren, M.; Tormod, S.; Tuzar, Z. 373 Rates of Association and Dissociation of Block Copolymer Micelles: 374 Light-Scattering Stopped-Flow Measurements. Makromol. Chem., 375 Rapid Commun. 1988, 9, 785-790.
- (12) Kositza, M. J.; Bohne, C.; Hatton, T. A.; Holzwarth, J. F. 377 Micellization Dynamics of Poly(Ethylene Oxide)-Poly(Propylene 378 Oxide)-Poly(Ethylene Oxide) Block Copolymers Measured by 379 Stopped Flow. Prog. Colloid Polym. Sci. 1999, 112, 146-151.
- (13) Wang, Y.; Balaji, R.; Quirk, R. P.; Mattice, W. L. Detection of 381 the Rate of Exchange of Chains between Micelles Formed by Diblock 382 Copolymers in Aqueous Solution. Polym. Bull. 1992, 28, 333-338. 383
- (14) Choi, S.-H.; Bates, F. S.; Lodge, T. P. Molecular Exchange in 384 Ordered Diblock Copolymer Micelles. Macromolecules 2011, 44 (9), 385 3594 - 3604
- (15) Ma, Y.; Lodge, T. P. Chain Exchange Kinetics in Diblock 387 Copolymer Micelles in Ionic Liquids: The Role of γ . Macromolecules 388 2016, 49 (24), 9542-9552.
- (16) Zhao, D.; Ma, Y.; Wang, E.; Lodge, T. P. Micellization of 390 Binary Diblock Co-Polymer Mixtures in an Ionic Liquid. Macro- 391 molecules 2019, 52 (12), 4729-4738.
- (17) Lund, R.; Willner, L.; Pipich, V.; Grillo, I.; Lindner, P.; 393 Colmenero, J.; Richter, D. Equilibrium Chain Exchange Kinetics of 394 Diblock Copolymer Micelles: Effect of Morphology. Macromolecules 395 **2011**, 44 (15), 6145–6154.
- (18) Won, Y.-Y.; Davis, H. T.; Bates, F. S. Molecular Exchange in 397 PEO-PB Micelles in Water. Macromolecules 2003, 36 (3), 953-955. 398
- (19) Willner, L.; Poppe, A.; Allgaier, J.; Monkenbusch, M.; Richter, 399 D. Time-resolved SANS for the Determination of Unimer Exchange 400 Kinetics in Block Copolymer Micelles. Europhys. Lett. 2001, 55, 667. 401
- (20) Wang, E.; Zhu, J.; Zhao, D.; Xie, S.; Bates, F. S.; Lodge, T. P. 402 Effect of Solvent Selectivity on Chain Exchange Kinetics in Block 403 Copolymer Micelles. Macromolecules 2020, 53 (1), 417-426.
- (21) Zhao, D.; Ma, Y.; Lodge, T. P. Exchange Kinetics for a Single 405 Block Copolymer in Micelles of Two Different Sizes. Macromolecules 406 2018, 51 (6), 2312-2320.
- (22) Cooksey, T. J.; Singh, A.; Le, K. M.; Wang, S.; Kelley, E. G.; 408 He, L.; Vajjala Kesava, S.; Gomez, E. D.; Kidd, B. E.; Madsen, L. A.; 409 Robertson, M. L. Tuning Biocompatible Block Copolymer Micelles 410 by Varying Solvent Composition: Core/Corona Structure and Solvent 411 Uptake. Macromolecules 2017, 50 (11), 4322-4334.
- (23) Zinn, T.; Willner, L.; Lund, R.; Pipich, V.; Richter, D. 413 Equilibrium Exchange Kinetics in N-Alkyl-PEO Polymeric Micelles: 414 Single Exponential Relaxation and Chain Length Dependence. Soft 415 Matter 2012, 8 (3), 623-626.
- (24) Lu, J.; Choi, S.; Bates, F. S.; Lodge, T. P. Molecular Exchange 417 in Diblock Copolymer Micelles: Bimodal Distribution in Core-Block 418 Molecular Weights. ACS Macro Lett. 2012, 1 (8), 982-985.

- 420 (25) Lu, J.; Bates, F. S.; Lodge, T. P. Addition of Corona Block
- 421 Homopolymer Retards Chain Exchange in Solutions of Block
- 422 Copolymer Micelles. Macromolecules 2016, 49 (4), 1405-1413.
- 423 (26) Kim, S.; Lee, S.; Choi, S.-H.; Char, K. Chain Exchange Kinetics
- 424 of Bottlebrush Block Copolymer Micelles. *Macromolecules* **2021**, 54
- 425 (10), 4739–4746.
- 426 (27) von Gottberg, F. K.; Smith, K. A.; Hatton, T. A. Dynamics of
- 427 Self-Assembled Surfactant Systems. J. Chem. Phys. 1998, 108 (5),
- 428 2232-2244.
- 429 (28) Cavicchi, K. A.; Lodge, T. P. Self-Diffusion and Tracer
- 430 Diffusion in Sphere-Forming Block Copolymers. *Macromolecules* 431 **2003**, 36, 7158–7164.
- 432 (29) Yokoyama, H.; Kramer, E. J. Self-diffusion of Asymmetric
- 433 Diblock Copolymers with a Spherical Domain Structure. *Macro-*434 molecules **1998**, 31, 7871–7876.
- 435 (30) Yokoyama, H.; Kramer, E. J. Diffusion of Triblock Copolymers
- 436 in a Spherical Domain Structure. Macromolecules 2000, 33, 954-959.
- 437 (31) Español, P.; Warren, P. Statistical Mechanics of Dissipative 438 Particle Dynamics. *Europhys. Lett.* **1995**, 30 (4), 191–196.
- 439 (32) Groot, R. D.; Warren, P. B. Dissipative Particle Dynamics:
- 440 Bridging the Gap between Atomistic and Mesoscopic Simulation. J.
- 441 Chem. Phys. 1997, 107 (11), 4423-4435.
- 442 (33) Li, Z.; Dormidontova, E. E. Kinetics of Diblock Copolymer
- 443 Micellization by Dissipative Particle Dynamics. *Macromolecules* **2010**,
- 444 43 (7), 3521–3531.
- 445 (34) Li, Z.; Dormidontova, E. E. Equilibrium Chain Exchange
- 446 Kinetics in Block Copolymer Micelle Solutions by Dissipative Particle
- 447 Dynamics Simulations. Soft Matter 2011, 7 (9), 4179.
- 448 (35) Peters, A. J.; Lodge, T. P. Chain Exchange Kinetics of
- 449 Asymmetric B₁AB₂ Linear Triblock and AB₁B₂ Branched Triblock
- 450 Copolymers. *Macromolecules* **2017**, 50 (16), 6303–6313.
- 451 (36) He, Y.; Li, Z.; Simone, P.; Lodge, T. P. Self-Assembly of Block
- 452 Copolymer Micelles in an Ionic Liquid. J. Am. Chem. Soc. 2006, 128 453 (8), 2745–2750.
- 454 (37) Amann, M.; Willner, L.; Stellbrink, J.; Radulescu, A.; Richter, D.
- 455 Studying the concentration dependence of the aggregation number of
- 456 a micellar model system by SANS. Soft Matter 2015, 11, 4208-4217.
- 457 (38) Fiorin, G.; Klein, M. L.; Hénin, J. Using Collective Variables to
- 458 Drive Molecular Dynamics Simulations. *Mol. Phys.* **2013**, *111* (22–459 23), 3345–3362.
- 460 (39) Plimpton, S. Fast Parallel Algorithms for Short-Range 461 Molecular Dynamics. *J. Comput. Phys.* **1995**, *117* (1), 1–19.
- 462 (40) Zhu, F.; Hummer, G. Convergence and error estimation in free
- 463 energy calculations using the weighted histogram analysis method. *J.*
- 464 Comput. Chem. 2012, 33 (4), 453-465.
- 465 (41) Grossfield, A. An Implementation of WHAM: The Weighted 466 Histogram Analysis Method Version 2.0.10.20.
- 467 (42) Kumar, S.; Rosenberg, J. M.; Bouzida, D.; Swendsen, R. H.;
- 468 Kollman, P. A. The Weighted Histogram Analysis Method for Free-
- 469 Energy Calculations on Biomolecules. I. The Method. J. Comput.
- 470 Chem. 1992, 13 (8), 1011-1021.
- 471 (43) Roy, S.; Bagchi, B. Free Energy Barriers for Escape of Water 472 Molecules from Protein Hydration Layer. J. Phys. Chem. B 2012, 116,
- 473 2958-2968.
- 474 (44) Mandal, T.; Koenig, P. H.; Larson, R. G. Nonmonotonic
- 475 Scission and Branching Free Energies as Functions of Hydrotrope
- 476 Concentration for Charged Micelles. Phys. Rev. Lett. 2018, 121, 477 030081.
- 478 (45) Wen, B.; Bai, B.; Larson, R. G. Surfactant desorption and 479 scission free energies for cylindrical and spherical micelles from
- 480 umbrella-sampling molecular dynamics simulations. J. Colloid Interface
- 481 Sci. 2021, 599, 773-784.
- 482 (46) Choi, S.-H.; Lodge, T. P.; Bates, F. S. Mechanism of Molecular
- 483 Exchange in Diblock Copolymer Micelles: Hypersensitivity to Core
- 484 Chain Length. Phys. Rev. Lett. 2010, 104, 047802.
- 485 (47) Guo, J.; Liang, H.; Wang, Z. Coil-to-globule transition by 486 dissipative particle dynamics simulation. *J. Chem. Phys.* **2011**, *134*,
- 487 244904.